



## A global compilation of coccolithophore calcification rates

Chris J. Daniels<sup>1</sup>, Alex J. Poulton<sup>1,2</sup>, William M. Balch<sup>3</sup>, Emilio Marañón<sup>4</sup>, Tim Adey<sup>5</sup>, Bruce C. Bowler<sup>3</sup>, Pedro Cermeño<sup>6</sup>, Anastasia Charalampopoulou<sup>5</sup>, David W. Crawford<sup>7,8</sup>, Dave Drapeau<sup>3</sup>, Yuanyuan Feng<sup>9</sup>, Ana Fernández<sup>4</sup>, Emilio Fernández<sup>4</sup>, Glauca M. Frago<sup>10</sup>,  
5 Natalia González<sup>11</sup>, Lisa M. Graziano<sup>3</sup>, Rachel Heslop<sup>5</sup>, Patrick M. Holligan<sup>5</sup>, Jason Hopkins<sup>3</sup>,  
María Huete-Ortega<sup>12</sup>, David A. Hutchins<sup>13</sup>, Phoebe J. Lam<sup>14</sup>, Michael S. Lipsen<sup>15</sup>, Daffne C. López-Sandoval<sup>16</sup>, Socratis Loucaides<sup>1,5</sup>, Adrian Marchetti<sup>17</sup>, Kyle M.J. Mayers<sup>5</sup>, Andrew P. Rees<sup>18</sup>, Cristina Sobrino<sup>4</sup>, Eithne Tynan<sup>5</sup>, Toby Tyrrell<sup>5</sup>.

10 <sup>1</sup> National Oceanography Centre, Southampton, SO14 3ZH, UK

<sup>2</sup> The Lyell Centre for Earth and Marine Sciences and Technology, Heriot-Watt University, Edinburgh, EH14 4AS, UK

<sup>3</sup> Bigelow Laboratory for Ocean Sciences, East Boothbay, ME 04544, Maine, USA

<sup>4</sup> Departamento de Ecología y Biología Animal, Universidad de Vigo, 36310 Vigo, Spain

15 <sup>5</sup> Ocean and Earth Science, National Oceanography Centre Southampton, University of Southampton, SO14 3ZH, UK

<sup>6</sup> Institut de Ciències del Mar, CSIC, E-08003 Barcelona, Spain

<sup>7</sup> Climate Chemistry Laboratory, Institute of Ocean Sciences, Fisheries and Oceans Canada, P.O. Box 6000, Sidney, BC, Canada

20 <sup>8</sup> Department of Biology, University of Victoria, Victoria, British Columbia BC V8P 5C2, Canada

<sup>9</sup> Tianjin University of Science and Technology, Tianjin Shi, 300457, China

<sup>10</sup> Trondhjem biological station, Department of Biology, Norwegian University of Science & Technology, NO-7491 Trondheim, Norway

<sup>11</sup> Biodiversity and Conservation Area, Universidad Rey Juan Carlos, E-28933 Madrid, Spain

25 <sup>12</sup> Department of Plant Sciences, University of Cambridge, CB2 3EA, UK

<sup>13</sup> Department of Biological Sciences, University of Southern California, Los Angeles, CA 90089, USA

<sup>14</sup> Department of Ocean Sciences, University of California, Santa Cruz, California, CA 95064, USA

<sup>15</sup> University of British Columbia, Department of Botany, Vancouver, British Columbia BC V6T 1Z4, Canada

30 <sup>16</sup> Red Sea Research Center, King Abdullah University of Science and Technology, Thuwal 23955-6900, Saudi Arabia

<sup>17</sup> Department of Marine Sciences, University of North Carolina at Chapel Hill, North Carolina, NC 27599, USA

<sup>18</sup> Plymouth Marine Laboratory, Prospect Place, West Hoe, Plymouth, PL1 3DH, UK

Correspondence to: Alex J. Poulton ([a.poulton@hw.ac.uk](mailto:a.poulton@hw.ac.uk))

35

**Abstract.** The biological production of calcium carbonate (CaCO<sub>3</sub>), a process termed calcification, is a key term in the marine carbon cycle. A major planktonic group responsible for such pelagic CaCO<sub>3</sub> production (CP) are the coccolithophores, single-celled haptophytes that inhabit the euphotic zone of the ocean. Satellite-based estimates of areal CP are limited to open-ocean waters, with current algorithms utilising the unique optical properties of the cosmopolitan bloom-forming species *Emiliania huxleyi*, whereas little understanding of the optical properties and environmental responses by species other than *E. huxleyi* are currently available to parameterise algorithms or models. To aid future areal estimations and validate future modelling efforts we have  
40



constructed a database of 2765 CP measurements, the majority of which were measured using 12 to 24 h  
incorporation of radioactive carbon ( $^{14}\text{C}$ ) into acid-labile inorganic carbon ( $\text{CaCO}_3$ ). We present data collated  
45 from over 30 studies covering the period from 1991 to 2015, sampling the Atlantic, Pacific, Indian, Arctic and  
Southern oceans. Globally, CP in surface waters (<20 m) ranged from 0.01 to 8398  $\mu\text{mol C m}^{-3} \text{d}^{-1}$  (with a  
geometric mean of 16.1  $\mu\text{mol C m}^{-3} \text{d}^{-1}$ ). An integral value for the upper euphotic zone (herein surface to the depth  
of 1% surface irradiance) ranged from <0.1 to 6  $\text{mmol C m}^{-2} \text{d}^{-1}$  (geometric mean 1.19  $\text{mmol C m}^{-2} \text{d}^{-1}$ ). The full  
database is available for download from PANGAEA as doi: 10.1594/PANGAEA.888182.

50

**Keywords.** Calcification, coccolithophores,  $\text{CaCO}_3$  production.

## 1 Introduction

The formation, export and burial of  $\text{CaCO}_3$  is an important component of the oceanic carbon cycle, with the  
55 combination of the first two providing a positive feedback on atmospheric  $\text{CO}_2$  (Archer, 1996; Sarmiento et al.,  
2002; Berelson et al. 2007). Around half of oceanic  $\text{CaCO}_3$  production occurs in shallow neritic environments,  
with the remainder occurring in the upper waters of the open-ocean (Milliman, 1993). Export and deep-sea burial  
in the open-ocean are both relatively well characterised in terms of global magnitude (Milliman, 1993; Berelson  
et al., 2007) and regional trends (e.g. Archer, 1996; Henson et al., 2012), and are often (simply) parameterised in  
60 global biogeochemical models (e.g. Gehlen et al., 2007; Yool et al., 2013) as a function of carbonate chemistry.  
The scale of biological formation of  $\text{CaCO}_3$  in the upper ocean, however, is poorly constrained, in terms of both  
its magnitude and biogeography (Berelson et al., 2007), due to knowledge gaps existing in the ecological and  
physiological understanding which is fundamental to allow accurate or reliable parameterisation at a global scale  
(Balch et al., 2007; Monteiro et al., 2016; Hopkins and Balch, 2018).

65

Problems with forming such a global perspective on pelagic  $\text{CaCO}_3$  production partly arise due to the diversity of  
the different planktonic organisms involved (coccolithophores, foraminifera, pteropods, and, to a lesser extent  
some dinoflagellates (Meier et al., 2007) and cyanobacteria (Merz-Preiß, 2000)), as well as our incomplete  
understanding of their ecology and physiology and a lack of *in situ* global measurements. Despite recent advances  
70 in understanding the biomass distribution of coccolithophores and foraminifera (O'Brien et al., 2013, 2016;  
Schiebel and Movellan, 2012), and how these may relate to carbonate chemistry (e.g. Bach et al., 2015; Evans et  
al., 2016), we still have very little idea of the relative magnitude (or biogeography) of their respective rates in  
terms of production or export (e.g. Schiebel, 2002; Berelson et al., 2007).

75 A key misconception when considering oceanic  $\text{CaCO}_3$  production by coccolithophores is the enigmatic role of  
*Emiliania huxleyi* in satellite imagery of  $\text{CaCO}_3$  (or particulate inorganic carbon, PIC). The characteristic light  
scattering properties of PIC particles, the size of *E. huxleyi* coccoliths (Balch et al., 1996), in addition to its  
ubiquitous distribution, tendency to shed excess coccoliths, and propensity to form massive turbid blooms, has set  
the focus on this species in the development of algorithms for satellite ocean-colour remote sensing of PIC  
80 measurements (Balch et al., 2005). Several studies have used satellite images to examine trends in global PIC  
production, in terms of regional variability, areal magnitude (e.g. Balch et al., 2005, 2007; Freeman and



Lovenduski, 2015; Hopkins and Balch, 2018) and coccolithophore ecology (e.g. Hopkins et al., 2015). However, these budgets are likely to be less accurate in terms of fully accounting for PIC contributions from the whole coccolithophore assemblage due to their diversity in coccolith-specific backscattering coefficients (Balch et al., 85 1999), which arise due to considerable diversity in coccolith sizes, shapes, morphologies and CaCO<sub>3</sub> contents (Young and Ziveri, 2000; Young et al., 2003). Relatively small differences in the CaCO<sub>3</sub> content of the various *E. huxleyi* morphotypes (Young et al., 2003; Poulton et al., 2011) can have significant impact in terms of CaCO<sub>3</sub> formation at the scale of mesoscale blooms (Poulton et al., 2013). Moreover, recent studies have highlighted the potential for less abundant, yet more heavily calcified species other than *E. huxleyi* to dominate coccolithophore 90 CaCO<sub>3</sub> production (Daniels et al., 2014, 2016), and hence there is a need to better consider community-wide CaCO<sub>3</sub> production. Satellites also detect relatively localised bloom events, whereas the non-bloom production in temperate waters may be relatively substantial (e.g. Poulton et al., 2010). Moreover, the areal extent of mid- to low-latitude waters confers them with a substantial global role in integrated CaCO<sub>3</sub> budgets (e.g. Balch et al., 2005; Marañón et al., 2016).

95

Here we focus on the pelagic CaCO<sub>3</sub> production (CP) from the global ocean, taking advantage of a recent increase in the oceanic measurement of their calcification rates across diverse ocean environments. As almost all coccolithophore species, with a few notable exceptions (Young et al., 1999), produce the calcite form of CaCO<sub>3</sub>, the terms CaCO<sub>3</sub> production and calcite production may be considered interchangeable for coccolithophores. 100 However, it also has to be noted that the methodology (see Sect. 2.1.2) to determine CP does not distinguish the *actual* form of CaCO<sub>3</sub>, whether it is calcite (coccolithophores, foraminifera, some dinoflagellates) or aragonite (foraminifera, pteropods, corals).

The ecology and physiology of coccolithophores has been reviewed numerous times (see Paasche, 2002; 105 Zondervan, 2007; Boyd et al., 2010; Raven and Crawford, 2012; Monteiro et al., 2016; Taylor et al., 2016). Recent advances also include a better understanding of coccolithophore calcification in the context of carbonate chemistry (Bach et al., 2015), energetic considerations (Monteiro et al., 2016) and phytoplankton succession (Hopkins et al., 2015). To date only two studies have previously collated and synthesised calcification rates across the global ocean (Balch et al., 2007; Poulton et al., 2007); however, there are now numerous studies published over the last 110 decade (see Table 1), which reformulates the global perspective on CP by coccolithophores. Poulton et al. (2007) previously noted a significant geographical bias in the data collected, with most data originating from (sub-)tropical waters, whereas measurements are now available from more diverse regions, such as the Arctic (e.g. Charalampopoulou et al., 2011; Balch et al., 2014; Daniels et al., 2016) and Southern Ocean (e.g. Balch et al., 2016; Charalampopoulou et al., 2016).

115

Paasche (1962, 1963) first proposed direct measurements of coccolithophore production of CaCO<sub>3</sub> by demonstrating that radioactive carbon-14 (<sup>14</sup>C) could trace the production of both organic (via photosynthesis) and inorganic carbon (via calcification) by coccolithophores in the laboratory. The use of <sup>14</sup>C to measure photosynthesis dates back to Steeman Nielsen in the 1950s (see Barber and Hilting, 2002), with a key step being 120 the acid-treatment of filtered material (post-incubation) to remove any remaining <sup>14</sup>C-labelled dissolved inorganic



carbon ( $^{14}\text{C}$ -DIC) as  $^{14}\text{CO}_2$  (e.g. Knap et al., 1996; Marra, 2002). However, if the filtered samples are rinsed (extensively) with unlabelled seawater to remove any unfixed  $^{14}\text{C}$ -DIC before acid exposure, then the  $^{14}\text{CO}_2$  liberated upon acidification of the filters represents  $^{14}\text{C}$ -DIC fixed into  $\text{Ca}^{14}\text{CO}_3$  (i.e. CP).

125 Two techniques exist to utilise this production of  $^{14}\text{CO}_2$  to measure calcification. The first requires filtering  $^{14}\text{C}$ -  
labelled samples post-incubation through two filters; one is then fumed with acid (e.g. hydrochloric acid) to  
remove the  $\text{Ca}^{14}\text{CO}_3$  (and then termed particulate organic production), while the other is left un-fumed (termed  
total particulate production). Calcification (particulate inorganic production) then represents the difference  
between the particulate production of these two filters. This “difference” method was first used in culture  
130 experiments (Paasche, 1963) and then later at sea by Balch et al. (1992) in the Gulf of Maine, while Fernández et  
al. (1993) used this technique to characterise  $\text{CaCO}_3$  production within an extensive bloom of coccolithophores  
in the North Atlantic. The second method (the ‘micro-diffusion technique’, MDT) directly captures the  $^{14}\text{CO}_2$   
liberated from  $\text{Ca}^{14}\text{CO}_3$ , providing a direct measurement of calcification with a high degree of accuracy. The MDT  
was originally developed by Paasche and Brubak (1994) and modified by Balch et al. (2000) for ship-based  
135 research, and has now been used in numerous field studies (see Table 1).

The objective of this study was to create a database compiling all the available *in situ* measurements of  $\text{CaCO}_3$   
production in the ocean. By synthesising the numerous individual datasets into one database, we hope to provide  
a baseline for validation of model outputs and satellite algorithms. Two previous data syntheses (Balch et al.,  
140 2007; Poulton et al., 2007) were published around a decade ago, though the datasets included were smaller with  
some geographical biases (i.e. a large amount of (sub-)tropical data): the present dataset aims to synthesise *all* the  
available calcification rate data, and will be updated as new data becomes available.

## 2 Data and Methods

145 The database is available at PANGAEA as doi: 10.1594/PANGAEA.888182 (Poulton et al., 2018).

### 2.1 Database construction

#### 2.1.1 Database summary

Data were compiled from the available scientific literature, with permission to include each dataset acquired from  
150 the lead author and/or principal investigator where appropriate. Following the initial data collection,  
oceanographic cruises with unpublished data were identified, and the data owners and originators contacted for  
permission and access to include those further datasets. The data consist of direct measurements of  $\text{CaCO}_3$   
production (CP) and primary production (PP), cell counts of coccolithophores (where available, not differentiated  
by species in this database), and ancillary data, including the collection date and year, latitude, longitude, sampling  
155 and light depth (when available), incubation length ( $\leq 12$  or 24 h) and method of measuring CP (via ‘difference’  
or MDT). The quality-controlled (see Sect. 2.2) database consists of 2765 data points, with coccolithophore cell  
counts matched to 1301 data points.



### 2.1.2 Calcium carbonate production and primary production

160  $\text{CaCO}_3$  production (CP) was mostly measured using  $^{14}\text{C}$ , with one study using  $^{45}\text{Ca}$  as a tracer (Van der Wal et al., 1995) (Table 1). Water samples (<0.5 L) were collected via various methods (e.g. Go-Flo bottles, Niskin bottles with rosette samplers, uncontaminated surface seawater supply), spiked with various activities (~2 to 100  $\mu\text{Ci}$  or ~74 to 3700 kBq) of  $^{14}\text{C}$ -labelled bicarbonate and incubated for 6 to 24 h under various light regimes (see original references in Table 1 for full methodological details). As CP is measured on small volumes (<0.5 L), with  
165 coccolithophore abundances ranging from 10 to 2000 cells  $\text{mL}^{-1}$ , such measurements are likely, but not exclusively, to exclude CP from large (63-200  $\mu\text{m}$ ) and rare calcifying organisms, such as foraminifera (typically  $\leq 0.01 \text{ mL}^{-1}$  or  $\leq 10 \text{ L}^{-1}$ ) or pteropods (typically  $\leq 0.001 \text{ mL}^{-1}$  or  $\leq 1 \text{ L}^{-1}$ ).

Two techniques were used with  $^{14}\text{C}$ : the 'difference' method and the MDT (Table 1). For measurements by  
170 'difference', the incubations are terminated by filtering the sample onto two replicate filters. One filter is fumed with acid (most often hydrochloric acid) to remove the acid-labile inorganic carbon (i.e.  $\text{CaCO}_3$ ), leaving non-acid labile particulate organic carbon, while the other is untreated. The radioactivity of the two filters is measured using liquid scintillation counting to determine the total carbon fixation (inorganic + organic carbon fixation, often termed total particulate production) on the untreated filter and the organic carbon fixation (often termed primary  
175 production, PP) on the acid-fumed filter.  $\text{CaCO}_3$  production is then determined as the difference between these two measurements. This technique can provide accurate estimates of CP when rates are high (and ratios of CP to PP are near unity), such as in coccolithophore blooms (e.g. Fernandez et al., 1993) or laboratory cultures (e.g. Balch et al., 1992). However, the accuracy of this technique suffers significantly in oceanic samples where CP can be much smaller than PP (less than a tenth of PP; Poulton et al., 2007), such that CP is calculated as the  
180 difference between two large numbers with potentially large errors (see Appendix A).

The MDT overcomes the limitations of the difference method, as it is able to measure directly both CP and PP from the same water sample, using only one filter (Balch et al., 2000; Paasche and Brubak, 1994). Following the incubation of seawater spiked with  $^{14}\text{C}$ -bicarbonate, the sample is filtered and extensively rinsed with non-labelled  
185 pre-filtered seawater, and the filter is placed into a glass vial. A glass fibre filter (e.g. Whatman GFA), pre-soaked with an alkaline solution (Balch et al., 2000) or  $\beta$ -phenylethylamine (Poulton et al., 2006; Balch et al., 2011) is suspended within the vial to act as a  $\text{CO}_2$  trap. The sample filter is then acidified (e.g. 1% phosphoric acid; see Balch et al., 2000), liberating the acid-labile inorganic carbon ( $\text{CaCO}_3$ ) as  $\text{CO}_2$ . The resultant  $^{14}\text{CO}_2$  is captured on the glass fibre filter over time (>12 h), which is then moved to a fresh vial from which CP can be measured  
190 directly. Measuring CP and PP from the same filter allows the MDT to reduce experiment error, resulting in more precise, reliable and accurate measurements of CP (Marañón and González, 1997; Balch et al., 2000, 2007). As a measure of abiotic isotope labelling of material, a formalin-killed blank incubation is run in parallel to the 'light' samples, and later subtracted (Balch et al., 2000).

195 An alternative method for measuring CP is through using  $^{45}\text{Ca}$  as the tracer rather than  $^{14}\text{C}$  (Van der Wal et al., 1995). Seawater is incubated with  $^{45}\text{CaCl}$  and subsequently filtered. The advantage of this method is that it does not require the separation of inorganic and organic uptake, as required for either  $^{14}\text{C}$  technique. However,  $^{45}\text{Ca}$



forms strong ionic bonds, such that unincorporated  $^{45}\text{Ca}$  is not easily removed by rinsing and blanks are often large (Balch et al., 2007; Van der Wal et al., 1995).

200

With the ability to measure low rates of CP, the MDT is the currently preferred method for measuring CP in the ocean, compared to both the “difference” method and  $^{45}\text{Ca}$ . This is reflected in the database, where 2527 (91.4 %) of the data points were measured using the MDT, 215 (7.8 %) using the difference technique, and 23 (0.8 %) using  $^{45}\text{Ca}$ . For a comparison of the performance of the MDT and the difference technique on oceanic coccolithophore communities see Appendix A.

205

The majority of the data in the current database comes from 24 h incubations, which captures a complete daily cycle of growth, and accounts for any CP (or loss of fixed carbon via mortality) occurring at night (Poulton et al., 2007, 2010). However, several earlier studies used shorter incubation lengths, and are highlighted in Table 1. The measurements collected by Poulton et al. (2006, 2007) were only incubated over the local daylight period (10-16 h), and it was assumed that negligible CP occurred at night (e.g. Linschooten et al., 1991; but see Paasche, 1966; Balch et al., 1992). Samples collected in the Gulf of Maine (Balch et al., 2008) were brought back to the laboratory to measure photosynthesis and CP in half-day, ‘CalCOFI-style’ (California Cooperative Oceanic Fisheries Investigations) incubations (see Mantyla et al., 1995). The half-day incubations minimised bottle effects (Balch et al., 2008), ran from local apparent midnight to midday, and were converted to daily rates of CP using ratios of 12 and 24 h incubations. Finally, Lam et al. (2001) incubated for 5 h around midday and calculated an hourly rate of CP. In this database, this hourly rate has been scaled up by the calculated day-length based on latitude, longitude and seasonal timing of the study (see Kirk, 1994), assuming that no dark calcification occurred, although this has been observed in laboratory cultures (Paasche, 1966; Linschooten et al., 1991; Balch et al., 1992). When appropriate, CP and PP data were standardised into units of  $\text{mmol C m}^{-3} \text{d}^{-1}$ .

210

215

220

### 2.1.3 Cell counts

When available, cell counts for coccolithophores (Table 1) were generally performed using either polarised light microscopy (Balch et al., 2004, 2008, 2012; Balch et al., unpublished; Daniels et al., 2016; Mayers et al., 2018; Mayers et al., unpublished; Poulton et al., 2010, 2013, 2014; Poulton et al., unpublished) or scanning electron microscopy (Charalampopoulou et al., 2011, 2016; Loucaides et al., unpublished; Poulton et al., unpublished). Other methods for cell counting in the database include inverted light microscopy of formalin-preserved samples (Lipsen et al., 2007; Marañón et al., 2016) and use of a haemocytometer (Marañón and González, 1997).

225

230

With the exception of Marañón and González (1997), who report only the concentration of *E. huxleyi*, cell counts correspond to the total concentration of coccolithophores in each water sample. In 556 of these samples, both the total coccolithophore abundance and the *E. huxleyi* abundance are reported (Charalampopoulou et al., 2011, 2016; Daniels et al., 2016; Lipsen et al., 2007; Loucaides et al., unpublished; Mayers et al., 2018.; Poulton et al., 2010, 2013; Poulton et al. unpublished). In all cases, the counts are reported in cells  $\text{mL}^{-1}$ .

235



#### 2.1.4 Optical depths, depth integration and surface data

240 There are 314 vertical profiles of CP within the database presented. From these profiles, depth-integrated values were calculated representing euphotic zone integrated CP (in which the euphotic zone is taken as either 1% of incident irradiance (e.g. Poulton et al., 2006) or 0.1% (e.g. Balch et al., 2011) in the different studies. Herein, it is assumed that CP only occurs within the euphotic zone and, therefore, euphotic zone integrated CP represents total water column CP by coccolithophores. Though coccolithophores may occur considerably deeper than the 1% irradiance depth (see e.g. Poulton et al., 2017), integration to the base of the euphotic zone allows comparison with other water-column processes frequently integrated to this depth (e.g. primary production, new production).

245 The light levels of the sampling depths, as a percentage of incident PAR, were provided either by the data originators or taken from the corresponding literature. Light depths were then converted to an equivalent optical depth by taking the negative natural logarithm approach where the 1% incident irradiance depth has an optical depth of 4.6 (see Kirk, 1994). The profiles were integrated by linearly interpolating using the sampling depths. There are 314 unique sampling stations with enough vertical resolution ( $n \geq 4$ ) to calculate euphotic zone integrals for CP (and PP) within the database.

255 However, a number of datasets included only upper ocean sampling and a subset of surface of data was created by extracting data collected from less than 20 m. In cases where multiple measurements were collected in this shallow window, only the data collected from the uppermost depth were extracted for the surface data comparison.

#### 2.2 Log normal distribution and quality control

260 Rates of CP and the abundance of coccolithophores in the ocean can range from zero when coccolithophores are either completely absent (e.g. in high latitude polar waters) or below the limit of detection, up to extremely high values that may occur, for example, in a coccolithophore bloom. Consequently, both the CP rates and cell abundances can vary over many orders of magnitude, exhibiting a log-normal distribution (Fig. 4A) when excluding zero-value data. This distribution is typical of many biological processes (Limpert et al., 2001). For log-normally distributed data the geometric mean, rather than arithmetic mean, best characterises the data and hence we report only the geometric means from the database.

265 We quality-controlled the datasets by first removing all negative CP values. Negative values can occur in the difference method as CP is significantly smaller than PP and when the variability (replication) in PP between filters can be greater than the CP signal (see Appendix A). A negative rate can also be obtained using the MDT if the formalin-killed blank is greater than the measured rates, as may occur at low light levels at the base of the euphotic zone (e.g. Poulton et al., 2010) or in water samples with low rates of CP. A negative rate of CP cannot actually occur using the (single point) radioisotope tracer technique and, therefore, these rates were eliminated from the database. The decision was also made to remove all zero-value data points of CP and cell counts. In general, the methods used to measure CP and cell abundances are not sensitive enough to distinguish between true zero values and those below their limit of detection. Furthermore, the limit of detection will vary between



275 users and specific details of their methods (e.g. volume used, spike activity added), and hence it is more consistent to remove all zero-values from the database rather than set an arbitrary limit of detection for the whole database.

### 3 Results and Discussion

#### 3.1 Data distribution

280 Figure 1 shows the spatial distribution of the database of CP. The Atlantic Ocean has the best data coverage, particularly in the high latitudes of the North Atlantic. Coverage of the Southern Ocean is constrained to the Atlantic and Indian Sectors. The Pacific Ocean is poorly represented with no coverage in the Western Pacific. Although there is a large number of data in the Indian Ocean, it is restricted to the Arabian Sea (Balch et al., 2000). The most heavily sampled region is the Gulf of Maine (Table 1) (Balch et al., 2008, 2012).

285 There are significant gaps in the spatial distribution of the dataset, with a particular bias towards the Atlantic Ocean. However, the spatial coverage has greatly increased since 2006 (see Balch et al., 2007; Poulton et al., 2007), particularly in the high latitudes. Figure 2 shows the temporal and seasonal distribution of the data. The increase in spatial coverage is partly attributable to the general increase in data collection, with 44% of the data collected since 2006. However, the seasonal distributions demonstrate bias towards the summer months of the 290 Northern (June – August) and Southern (December – February) hemispheres (Figs. 2B and 2C).

Figure 3 shows the vertical distribution of the database, in terms of depth and optical depth. Most data were collected from relatively shallow waters: 60% of samples were collected from less than 20 m, and 41% at more than 50% of surface irradiance (optical depths  $<0.7$ ).

295

#### 3.2 Magnitude of $\text{CaCO}_3$ production rates

The entire dataset of CP is well approximated by a log-normal distribution (Fig. 4A), with a geometric mean of  $16.1 \mu\text{mol C m}^{-3} \text{d}^{-1}$ . The total range in CP is from 0.01 to  $8398 \mu\text{mol C m}^{-3} \text{d}^{-1}$ , which has greatly expanded compared to Poulton et al. (2007). The highest measured CP rate occurred in the Gulf of Maine in July 2002 300 (Balch et al., 2012). Rates of CP in excess of  $5000 \mu\text{mol C m}^{-3} \text{d}^{-1}$  were measured twice in a coccolithophore bloom in the Celtic Sea in April 2015 (Mayers et al., 2018). In total, there are 23 occurrences of CP rates over  $1000 \mu\text{mol m}^{-3} \text{d}^{-1}$ , very likely indicative of coccolithophore blooms (Poulton et al., 2007, 2013).

##### 3.2.1 Surface $\text{CaCO}_3$ production

305 The surface CP data are also approximated by a log-normal distribution (Fig. 4B), with a slightly higher geometric mean ( $20.3 \mu\text{mol C m}^{-3} \text{d}^{-1}$ ) than the complete dataset. Surface CP spans the entire range in CP ( $0.01 - 8398 \mu\text{mol C m}^{-3} \text{d}^{-1}$ ), and is highly variable in the ocean (Fig. 5A). In general, surface CP is higher in the high latitude North Atlantic (Fernández et al., 1993; Poulton et al., 2010; Daniels et al., 2016), the Patagonian Shelf region of the South Atlantic (Poulton et al., 2013), the North Pacific (Lipsen et al., 2007) and in the Arabian Sea (Balch et al., 310 2000). Some of the lowest rates of CP are observed in the Southern Ocean (Charalampopoulou et al., 2016), although there is no clear pattern in the global distribution. The higher CP rates tend to be in well-sampled regions



as studies have targeted areas known or predicted to be areas of significant coccolithophore abundances. This geographical (and seasonal) sampling bias may have resulted in an inflated global mean value of CP as there are only a few data points from regions where coccolithophores are thought to be rare (e.g. the subtropical Pacific and high latitude polar seas).

### 3.2.2 Integrated CaCO<sub>3</sub> production

Integrated CP is also log-normally distributed, with a geometric mean of 1.19 mmol C m<sup>-2</sup> d<sup>-1</sup>, and a range of <0.01 to 6 mmol C m<sup>-2</sup> d<sup>-1</sup>. As there are significantly less vertical profiles of CP (314) than surface measurements of CP (1103), the spatial coverage of integrated CP is much sparser (Fig. 5B), particularly in the high latitude North Atlantic. The pattern of integrated CP is slightly different to that of surface CP. Although integrated CP is high on the Patagonian Shelf, in the Arabian Sea and in the sub-polar North Atlantic, it is also high in the Equatorial Pacific. This partly reflects the deeper euphotic zones (> 60 m) in the Equatorial Pacific compared to the sub-polar regions (< 50 m) (see Landry et al., 2011). The vertical distribution of CP against optical depth is shown in Fig. 4C. The lack of relationship between CP and optical depth for the entire dataset is partly due to the fact that the global variation in CP for any optical depth is greater than the vertical pattern in CP.

There is a strong positive correlation between surface CP and integrated CP (Pearson's product-moment correlation,  $r = 0.83$ ,  $p < 0.001$ ,  $n = 314$ ), when the logarithms of both are taken (Fig. 6). While a strong correlation between surface PP and integrated PP has been previously observed (e.g. Poulton et al., 2007), and is observed here (Fig. 7A), the relationship observed for CP by Poulton et al. (2007) was statistically weaker ( $r = 0.47$ ,  $p < 0.001$ ,  $n = 68$ ). This difference may relate to the greater degree of temperate data in the larger database, where light will be a strong driver of deep CP within the mixed layer. In contrast, the previous database had a greater degree of tropical data, where deep thermocline CP may be strongly light-limited and/or dependent on non-autotrophic nutrition (Poulton et al., 2017).

### 3.3 CaCO<sub>3</sub> production versus primary production

The ratio of CP to PP is highly variable in the database (Fig. 7A), with a log-normal distribution (Fig. 7B). The average (geometric mean) ratio of CP:PP for the total database is 0.02, though it has a range from as low as below 0.0001 to as high as over 5. This distribution is highly similar to that observed by Poulton et al. (2007), though there is a much greater degree of variability within the expanded dataset (and potential issues with the more extreme values).

Broadly similar trends are observed when considering both surface CP and PP (Fig. 7C) and integrated CP and PP (Fig. 7E), with average CP:PP around 0.01 and 0.03, respectively. As the average CP:PP ratio is lower in surface waters than in the total dataset, there may be a decoupling of PP and CP with depth and a greater light-dependency for photosynthesis than calcification (see Balch and Kilpatrick, 1996; Balch et al., 2000, 2011; Poulton et al., 2007, 2010). The effect of optical depth on the ratio of CP to PP is shown in Fig. 7D. No general trend is identifiable, with data from deeper optical depths having similar CP:PP ratios to surface values. CP at depths below the light levels required for photosynthesis may also relate to non-autotrophic nutritional strategies



by deep-dwelling coccolithophore species (e.g. Poulton et al., 2017). No clear relationship is found between latitude and CP:PP (Fig. 7F).

355 The log-normal relationship between CP and PP can be potentially useful in a practical sense. Oceanic rates of PP  
are much more widely measured in field programmes, and therefore PP is better constrained than CP. By using  
the log-normal relationship between CP and PP identified in the global database we may be able to gain greater  
insights into spatial and temporal patterns, as well as the extent of CP. For example, global marine PP is estimated  
to be  $\sim 50$  Gt C yr<sup>-1</sup> (Field et al., 1998) while global CP is poorly constrained with estimates ranging from 0.4 to 8  
Gt C yr<sup>-1</sup> (Balch et al., 2007; Berelson et al., 2007). A first order approximation of global CP, using the average  
360 CP:PP of 0.02 from the database, gives an estimate of  $\sim 1$  Gt C yr<sup>-1</sup>. This value is only slightly lower than a recent  
estimate, based on coccolithophore ecophysiology, of 1.42 Gt C yr<sup>-1</sup> by Hopkins and Balch (2018). Clearly, more  
sophisticated methods can also be used in the future with the global CP database to better approximate regional  
and global estimates of CP.

#### 365 3.4 Cell-normalised calcification

A key consideration in measurements of oceanic biogeochemical rates is the accuracy and representativeness of  
the resulting values. For PP (and photosynthesis), normalising rates to concentrations of chlorophyll-*a* (or  
phytoplankton carbon) gives information about the variability in production per unit biomass, where a solid  
understanding of photo-physiology (e.g. Behrenfeld and Falkowski, 1997; Falkowski and Raven, 1997) helps to  
370 identify physiologically unrealistic rates. In the case of CP, normalising to chlorophyll-*a* or particulate inorganic  
carbon (PIC) can be considered inappropriate, as neither of them fully represent living coccolithophore biomass  
(Poulton et al., 2007).

We suggest that a more physiologically sound approach is to normalise CP to coccolithophore cell abundance  
375 (Poulton et al., 2010; Fig. 8), which provides a measure of calcification per unit ‘biomass’ (cell-CP) comparable  
(in basic terms) to chlorophyll-normalised photosynthetic rates. Figure 8 shows the variability in cell-CP when  
normalising CP to total coccolithophore abundance using the matched values available in the database.

380 Within natural coccolithophore communities, CP is dependent on cell abundance, species composition and the  
rate of calcification per cell (Poulton et al., 2010; Daniels et al., 2014). Using cell-CP to examine coccolithophore  
dynamics is particularly appropriate when applied to communities dominated by a few species due to the  
sensitivity of cell-CP to cellular CaCO<sub>3</sub> content, and hence species composition (Poulton et al., 2010;  
Charalampopoulou et al., 2011). More recently it has also been modified to account for variability in growth rates  
and species composition, allowing species-specific contributions to community CP to be constrained (Daniels et  
385 al., 2016).

The values of cell-CP in Fig. 8 range from  $<0.001$  to 46.4 pmol C cell<sup>-1</sup> d<sup>-1</sup>, with a geometric mean of 0.42 pmol  
C cell<sup>-1</sup> d<sup>-1</sup> ( $n = 1272$ ). The cell-CP of *E. huxleyi* dominated natural communities is known to be variable, with



average reported field values ranging from 0.16 to 0.65 pmol C cell<sup>-1</sup> d<sup>-1</sup> across non-bloom communities in the  
390 North Atlantic and Southern Ocean, as well as bloom communities on the Patagonian Shelf (Poulton et al., 2010,  
2013; Charalampopoulou et al., 2016). A cell-CP of 0.023 pmol C cell<sup>-1</sup> d<sup>-1</sup>, equivalent to an *E. huxleyi* coccolith  
production rate of ~1 day<sup>-1</sup> (Young and Ziveri, 2000; Poulton et al., 2010), can be considered close to a theoretical  
minimum cell-CP for *E. huxleyi*. Thus, samples in Fig. 8 with a cell-CP lower than this value are likely to be  
dominated by coccolithophore species with much lower cellular CaCO<sub>3</sub> contents than *E. huxleyi* (e.g.  
395 *Calciopappus caudatus*; Daniels et al., 2016; Mayers et al., 2018). Conversely, those samples with a cell-CP  
significantly greater than 1 pmol C cell<sup>-1</sup> d<sup>-1</sup> are likely to be dominated by coccolithophore species with greater  
cellular contents than *E. huxleyi*. Cell-CP for heavily calcified coccolithophore species such as *Coccolithus*  
*pelagicus*, may reach as high as ~8.3 pmol cell<sup>-1</sup> d<sup>-1</sup> or ~23.2 pmol C cell<sup>-1</sup> d<sup>-1</sup> for *C. braarudii* (depending on the  
cell CaCO<sub>3</sub> content and growth rate; Daniels et al., 2014). A theoretical maximum could therefore be considered  
400 as ~40 pmol C cell<sup>-1</sup> d<sup>-1</sup>; based, for example, on a maximum growth rate of 0.6 d<sup>-1</sup> for the heaviest extant  
coccolithophore species (*Scyphosphaera apsteinii*; Young and Ziveri, 2000) with ~10 to 12 coccoliths per  
coccosphere (Young et al., 2003) and a cell CaCO<sub>3</sub> of ~54 to 65 pmol C cell<sup>-1</sup>.

The values of cell-CP in the CP database (Fig. 8) are mostly within these theoretical limits, indicating that they  
405 can be viewed as ‘realistic’ in the context of physiological limitations (growth and coccolith production rates) and  
extant species composition (cell and coccolith calcite quotas). Hence, cell-CP provides a useful benchmark for  
examining the physiological and growth dynamics of coccolithophore communities (e.g. Poulton et al., 2010,  
2013; Charalampopoulou et al., 2016; Daniels et al., 2016; Mayers et al., 2018), as well as acting as a reality check  
for oceanic measurements of CP. The relative species composition of mixed communities also has to be considered  
410 when examining trends in cell-CP (and total CP), which fittingly links together the biogeochemically important  
role of coccolithophores in CP with their diversity in form, function and ecophysiology.

#### 4 Conclusions and future recommendations

We have assembled a database of 2765 data points of CP across the global ocean (from oceanic to coastal and  
415 tropical to polar), resulting in a significant increase in both the size and the spatial coverage of previous syntheses  
of similar measurements (Balch et al., 2007; Poulton et al., 2007). This database may be valuable in global-scale  
studies of CP and coccolithophores, though the main limitations of the current database are its spatial coverage,  
with particularly poor coverage in the Pacific, and a significant temporal bias towards spring/summer sampling.

420 The CP data are log-normally distributed, such that geometric means are required for examining the CP data.  
There is significant variability in the CP data, with no clear patterns in the global distribution of either surface or  
integrated CP, although there is a strong relationship between surface CP and integrated CP. We recommend that  
future field studies of CP use the MDT technique in combination with cell counts to obtain estimates of cell-CP  
to ‘ground-truth’ the CP measurements. Cell-CP also provides further insights into the coccolithophore diversity  
425 and physiology underpinning measurements of CP. The MDT technique is the only direct method capable of  
accurately measuring low rates of CP (see Appendix A). The CP database is freely available and stored  
permanently at PANGAEA (Poulton et al., 2018; doi: 10.1594/PANGAEA.888182) and there are plans to update



it as and when new data becomes available. We hope that the database will be useful in model and satellite validation, and for examining spatial and temporal variability in CP on a global scale.

430

**Author contributions.** CJD and AJP devised the data synthesis and collated the data, with earlier assistance from RH. All authors contributed data to the database. WMB and EM commented on early drafts of the paper. All authors commented on subsequent drafts. KMJM and JH also assisted with the final versions of the figures.

435

**Competing interests.** The authors declare that they have no conflicts of interest.

**Acknowledgements.** The authors wish to thank the research scientists, technicians, students and crew who contributed to the collection of these data. The authors also recognise funding from the UK Natural Environmental Research Council (NERC), the US National Science Foundation (NSF), National Aeronautics and Space Administration (NASA), and the Spanish Ministry of Science and Innovation.

440

## References

Archer, D.E.: An atlas of the distribution of calcium carbonate in sediments of the deepsea, *Global Biogeochem. Cy.*, 10, 159-174, 1996.

445

Bach, L.T., Riebesell, U., Gutowska, M.A., Federwisch, L., and Schulz, K.G.: A unifying concept of coccolithophore sensitivity to changing carbonate chemistry embedded in an ecological framework, *Prog. Oceanogr.*, 135, 125-138, doi: 10.1016/j.pocean.2015.04.012, 2015.

450

Balch, W., Drapeau, D., Bowler, B., and Booth, E.: Prediction of pelagic calcification rates using satellite measurements, *Deep-Sea Res. II*, 54, 478-495, doi: 10.106/j.dsr2.2006.12.006, 2007.

455

Balch, W.M., Poulton, A.J., Drapeau, D., Bowler, B., Windecker, L., and Booth, E.: Zonal and meridional patterns of phytoplankton biomass and carbon fixation in the Equatorial Pacific Ocean, between 110°W and 140°W, *Deep-Sea Res. II*, 58, 400-416, doi: 10.1016/j.dsr2.2010.08.004, 2011.

460

Balch, W.M., Eppley, R.W., Abbott, M.R., and Reid, F.M.H.: Bias in satellite-derived pigment measurements due to coccolithophores and dinoflagellates, *J. Plank. Res.*, 11, 575-581, 1989.

465

Balch, W.M., Holligan, P.M., and Kilpatrick, K.A.: Calcification, photosynthesis and growth of the bloom-forming coccolithophore, *Emiliania huxleyi*, *Cont. Shelf Res.*, 12, 1353-1374, doi: 10.1016/0278-4343(92)90059-s, 1992.

470

Balch, W.M., and Kilpatrick, K.: Calcification rates in the Equatorial Pacific along 140°W, *Deep-Sea Res. II*, 43, 971-993, doi: 10.1016/0967-0645(96)00032-X, 1996.

475

Balch, W.M., Kilpatrick, K., Holligan, P.M., Harbour, D., and Fernandez, E.: The 1991 coccolithophore bloom in the central North Atlantic: 2. Relating optics to coccolith concentration, *Limnol. Oceanogr.* 41, 1684-1696, 1996.



- 475 Balch, W.M., Drapeau, D.T., Cucci, T.L., Vaillancourt, R.D., Kilpatrick, K.A., and Fritz, J.J.: Optical backscattering by calcifying algae – Separating the contribution by particulate inorganic and organic carbon fractions, *J. Geophys. Res.*, 104, 1541-1558, 1999.
- Balch, W.M., Drapeau, D.T., and Fritz, J.J.: Monsoonal forcing of calcification in the Arabian Sea, *Deep-Sea Res. II*, 47, 1301-1337, doi: 10.1016/S0967-0645(99)00145-9, 2000.
- 480 Balch, W.M., Drapeau, D.T., Bowler, B.C., Booth, E.S., Goes, J.I., Ashe, A., and Frye, J.M.: A multi-year record of hydrographic and bio-optical properties in the Gulf of Maine: I. Spatial and temporal variability, *Prog. Oceanogr.*, 63, 57-98, doi: 10.106/j.pcean.2004.09.003, 2004.
- Balch, W.M., Gordon, H.R, Bowler, C., Drapeau, D.T., and Booth, E.S.: Calcium carbonate measurements in the surface gloal ocean based on Moderate-Resolution Imaging Spectroradiometer data, *J. Geophys.Res.*, 110, C07001, doi: 10.1029/2004JC002560, 2005.
- 485 Balch, W.M., Drapeay, D.T., Bowler, B.C., Booth, E.S., Windecker, L.A., and Ashe, A.: Space-time variability of carbon standing stocks and fixation rates in the Gulf of Maine, along the GNATS transect between Portland, ME, USA and Yarmouth, Nova Scotia, Canada, *J. Plankton Res.*, 30, 119-139, doi: 10.1093/plant/fbm097, 2008.
- 490 Balch, W.M., Drapeau, D.T., Bowler, B.C., and Huntington, T.G.: Step-changes in the physical, chemical and biological characteristics of the Gulf of Maine, as documented by the GNATS time series, *Mar. Ecol. Prog. Ser.*, 450, 11-35, doi: 10.3354/meps09555, 2012.
- 495 Balch, W.M., Bowler, B.C., Lubelczyk, L.C., and Stevens Jr., M.W.: Aerial extent, composition, bio-optics and biogeochemistry of a massive under-ice algal bloom in the Arctic, *Deep-Sea Res. II*, 105, 42-58, doi: 10.1016/j.dsr2.2014.04.001, 2014.
- 500 Balch, W.M., Bates, N.R., Lam, P.J., Twining, B.S., Rosengard, S.Z., Bowler, B.C., Drapeau, D.T., Garley, R., Lubelczyk, L.C., Mitchell, C., and Rauschenberg, S.: Factors regulating the Great Calcite Belt in the Southern Ocean and its biogeochemical significance, *Global Biogeochem. Cy.*, 30, 1124-1144, doi: 10.1002/2016GB005414, 2016.
- 505 Barber, R.T., and Hilting, A.: History of the study of plankton productivity, In: *Phytoplankton productivity, carbon assimilation in marine and freshwater ecosystems* (Eds: Williams, P.K.le B., Thomas, D.N., and Reynolds, C.S.), Blackwell Science, 16-43, 2002.
- Behrenfeld, M.J., and Falkowski, P.G.: Photosynthetic rates derived from satellite-based chlorophyll concentration, *Limnol. Oceanogr.*, 42, 1-20, 1997.
- 510 Berelson, W.M., Balch, W.M., Najjar, R., Feely, R.A., Sabine, C., and Lee, K.: Relating estimates of CaCO<sub>3</sub> production, export, and dissolution in the water column to measurements of CaCO<sub>3</sub> rain into sediment traps and dissolution on the sea floor: A revised global carbonae budget, *Global Biogeochem. Cy.*, 21, doi: 10.1029/2006GB002803, 2007.
- 515 Boyd, P.W., Strzepek, R., Fu, F., and Hutchins, D.A.: Environmental control of open-ocean phytoplankton groups: Now and in the future, *Limnol. Oceanogr.*, 55, 1353-1376, doi: 10.4319/lo.2010.55.3.1353., 2010.
- 520 Charalampopoulou, A., Poulton, A.J., Tyrrell, T., and Lucas, M.I.: Irradiance and pH affect coccolithophore community composition on a transect between the North Sea and the Arctic Ocean, *Mar. Ecol. Prog. Ser.*, 431, 25-43, doi: 10.3354/meps09140, 2011.



- 525 Charalampopolou, A., Poulton, A.J., Bakker, D.C.E., Lucas, M.I., Stinchcombe, M.C., and Tyrrell, T.: Environmental drivers of coccolithophore abundance and calcification across Drake Passage (Southern Ocean), *Biogeosciences*, 13, 5917-5935, doi: 10.5194/bg-2016-139, 2016.
- Daniels, C.J., Sheward, R.M., and Poulton, A.J.: Biogeochemical implications of comparative growth rates of *Emiliania huxleyi* and *Coccolithus* species, *Biogeosciences*, 11, 6915-6925, doi: 10.5194/bg-11-6915-2014.
- 530 Daniels, C.J., Poulton, A.J., Young, J.R., Esposito, M., Humphreys, M.P., Ribas-Ribas, M., Tynan, E., and Tyrrell, T.: Species-specific calcite production reveals *Coccolithus pelagicus* as the key calcifier in the Arctic Ocean, *Mar. Ecol. Prog. Ser.*, 555, 29-47, doi: 10.3354/meps11820, 2016.
- 535 Delille, D., Harley, J., Zondervan, I., Jacquet, S., Chou, L., Wollast, R., Bellerby, R.G.J., Frankignoulle, M., Borges, A.V., Riebesell, U., and Gattuso, J-P.: Response of primary production and calcification to changes of pCO<sub>2</sub> during experimental blooms of the coccolithophorid *Emiliania huxleyi*, *Global Biogeochem. Cy.*, 19, doi: 10.1029/2004GB002318, 2015.
- 540 Evans, D., Wade, B.S., Henehan, M., Erez, J., and Müller, W.: Revisiting carbonate chemistry controls on planktic foraminifera Mg/Ca: implications for sea surface temperature and hydrology shifts over the Paleocene-Eocene Thermal Maximum and Eocene-Oligocene transition, *Clim. Past*, 12, 819-835, doi: 10.5194/cp-12-819-2016, 2016.
- 545 Falkowski, P.G., and Raven, J.A.: *Aquatic Photosynthesis*, Princeton University Press, first edition, 1997.
- Feng, Y., Hare, C.E., Leblanc, K., Rose, J.M., Zhang, Y., DiTullio, G.R., Lee, P., Wilhelm, S., Rowe, J.M., and Sun, J.: The effects of increased pCO<sub>2</sub> and temperature on the North Atlantic spring bloom: I. The phytoplankton community and biogeochemical response, *Mar. Ecol. Prog. Ser.*, 388, 13-25, doi: 10.3354/meps08133, 2009.
- 550 Fernandez, E., Boyd, P., Holligan, P.M., and Harbour, D.S.: Production of organic and inorganic carbon within a large-scale coccolithophore bloom in the northeast Atlantic Ocean, *Mar. Ecol. Prog. Ser.*, 97, 271-285, doi: 10.3354/meps097271, 1993.
- 555 Fernandez, E., Marañón, E., Harbour, D.S., Kristiansen, S., and Heimdal, B.: Patterns of carbon and nitrogen uptake during blooms of *Emiliania huxleyi* in two Norwegian fjords, *J. Plankton Res.*, 18, 2349-2366, 1996.
- Field, C.B., Behrenfeld, M.J., Randerson, J.T., and Falkowski, P.: Primary production of the Biosphere: Integrating terrestrial and oceanic components, *Science*, 281, 237-240, doi: 10.1126/science.281.5374.237, 1998.
- 560 Freeman, N.M., and Lovenduski, N.S.: Decreased calcification in the Southern Ocean over the satellite record, *Geophys. Res. Lett.*, 42, 1834-1840, doi: 10.1029/2014GL062769, 2015.
- 565 Gehlen, M., Ganstø, R., Schneider, B., Bopp, L., Aumont, O., and Ethe, C.: The fate of pelagic CaCO<sub>3</sub> production in a high CO<sub>2</sub> ocean: A model study, *Biogeosciences*, 4, 505-519, 2007.
- Henson, S.A., Sanders, R., and Madsen, E.: Global patterns in the efficiency of particulate organic carbon export and transport to the deep ocean, *Global Biogeochem. Cy.*, 26, doi: 10.1029/2011GB004099, 2012.
- 570 Hopkins, J., Henson, S.A., Painter, S.C., Tyrrell, T., and Poulton, A.J.: Phenological characteristics of global coccolithophore blooms, *Global Biogeochem. Cy.*, 29, 239-253, doi: 10.1002/2014GB004919, 2015.
- Hopkins, J., and Balch, W.M.: A new approach to estimating coccolithophore calcification rates from space, *J. Geophys. Res.*, in press, doi: 10.1002/2017JG004235, 2018.



- 575 Kirk, J.T.O.: Light and photosynthesis in aquatic ecosystems, Cambridge University Press, Cambridge, 1994.
- Knap, A.H., Michaels, A., Close, A.R., Ducklow, H., and Dickson, A.G.: Protocols for the Joint Global Ocean Flux Study (JGOFS) core measurements, JGOFS Report Nr. 19, IOC Manuals and Guides No. 29, UNESCO, 170, 1996.
- 580 Lam, P.J., Tortell, P.D., and Morell, F.M.M.: Differential effects of iron additions on organic and inorganic carbon production by phytoplankton, *Limnol. Oceanogr.*, 46, 1199-1202, doi: 10.4319/lo.2001.46.5.1199, 2001.
- 585 Landry, M.R., Selph, K.E., Taylor, A.G., Décima, M., Balch, W.M., and Bidigare, R.R.: Phytoplankton growth, grazing and production balances in the HNLC equatorial Pacific, *Deep-Sea Res. II*, 58, 524-535, 2011.
- Limpert, E., Stahel, W.A., and Abbt, M.: Log-normal distributions across the sciences: Keys and Clues: On the charms of statistics, and how mechanical models resembling gambling machines offer a link to a handy way to characterize log-normal distributions, which can provide deeper insights into variability and probability – normal or log-normal: That is the question, *Bioscience*, 51, 341-352, doi: 10.1641/0006-3568(2001)051[0341:LNDATS]2.0.CO;2, 2001.
- 590 or log-normal: That is the question, *Bioscience*, 51, 341-352, doi: 10.1641/0006-3568(2001)051[0341:LNDATS]2.0.CO;2, 2001.
- Linschooten, C., van Bleijswijk, J.D.L., Van Emburg, P.R., de Vrind, J.P.M., Kempers, E.S., Westbroek, P., and de Vrind-de Jong, E.W.: Role of the light-dark cycle and medium composition on the production of coccoliths by *Emiliania huxleyi* (haptophyceae), *J. Phycol.*, 27, 82-76, 1991.
- 595 Linschooten, C., van Bleijswijk, J.D.L., Van Emburg, P.R., de Vrind, J.P.M., Kempers, E.S., Westbroek, P., and de Vrind-de Jong, E.W.: Role of the light-dark cycle and medium composition on the production of coccoliths by *Emiliania huxleyi* (haptophyceae), *J. Phycol.*, 27, 82-76, 1991.
- Lipsen, M., Crawford, D., Gower, J., and Harrison, P.: Spatial and temporal variability in coccolithophore abundance and production of PIC and POC in the north-east subarctic Pacific during El Nino (1998), La Nina (1999) and 2000, *Prog. Oceanogr.*, 75, 304-325, doi: 10.1016/j.pocean.2007.08.004, 2007.
- 600 Lipsen, M., Crawford, D., Gower, J., and Harrison, P.: Spatial and temporal variability in coccolithophore abundance and production of PIC and POC in the north-east subarctic Pacific during El Nino (1998), La Nina (1999) and 2000, *Prog. Oceanogr.*, 75, 304-325, doi: 10.1016/j.pocean.2007.08.004, 2007.
- Mantyla, A.W., Venrick, E.L., and Hayward, T.L.: Primary production and chlorophyll relationships, derived from ten years of CalCOFI measurements, *CalCOFI Rep.*, 36, 159-166, 1995.
- 605 Marra, J.: Approaches to the measurement of plankton production, In: *Phytoplankton productivity: carbon assimilation in marine and freshwater ecosystems* (Eds: Williams, P.K. le B., Thomas, D.N., Reynolds, C.S.), Blackwell Science, 78-108, 2002.
- Marra, J., and Barber, R.T.: Phytoplankton and heterotrophic respiration in the surface layer of the ocean, *Geophys. Res. Lett.*, 31, L09314, doi: 10.1029/2004GL019664, 2004.
- 610 Marra, J., and Barber, R.T.: Phytoplankton and heterotrophic respiration in the surface layer of the ocean, *Geophys. Res. Lett.*, 31, L09314, doi: 10.1029/2004GL019664, 2004.
- Marañón, E., and Gonzalez, N.: Primary production, calcification and macromolecular synthesis in a bloom of the coccolithophore *Emiliania huxleyi* in the North Sea, *Mar. Ecol. Prog. Ser.*, 157, 61-77, doi: 10.3354/meps157061, 1997.
- 615 Marañón, E., Balch, W.M., Cermeño, P., González, N., Sobrino, C., Fernández, A., Huete-Ortega, M., López-Sandoval, D.C., Delgado, M., Estrada, M., Álvarez, M., Fernández-Guallart, E., and Pelejero, C.: Coccolithophore calcification is independent of carbonate chemistry in the tropical ocean, *Limnol. Oceanogr.*, 61, 1345-1357, doi: 10.1002/lno.10295, 2016.
- 620 Marchetti, A., Sherry, N.D., Juneau, P., Strzepek, R.F., and Harrison, P.J.: Phytoplankton processes during a mesoscale iron enrichment in the northeast Pacific: Part III. Primary productivity, *Deep-Sea Res. II*, 53, 2131-2151, doi: 10.1016/j.dsr2.2006.05.032, 2006.
- 625 Mayers, K.M.J., Poulton, A.J., Daniels, C.J., Wells, S.R., Woodward, E.M.S., Tarran, G.A., Widdicombe, C.E., Mayor, D.J., Atkinson, A., and Giering, S.L.C.: Growth and mortality dynamics of coccolithophores during spring in a temperate Shelf Sea (Celtic Sea, April 2016), *Prog. Oceanogr.*, in press, doi: 10.1016/j.pocean.2018.02.024, 2018.



- 630 Meier, K.J.S., Young, J.R., Kirsch, M., and Feist-Burkhardt, S.: Evolution of different life-cycle strategies in oceanic calcareous dinoflagellates, *Eur. J. Phycol.*, 42, 81-89, doi: 10.1080/09670260600937833, 2007.
- Merz-Preiß, M.: Calcification in cyanobacteria, In: *Microbial Sediments* (Eds. Riding, R.E., and Awramik, S.M.), Springer, Berlin, Heidelberg, 2000.
- 635 Milliman, J.D.: Production and accumulation of calcium carbonate in the ocean: Budget of a non-steady state, *Global Biogeochem. Cy.*, 7, 927-957, 1993.
- Monteiro, F.M., Bach, L.T., Brownlee, C., Brown, P., Rickaby, R.E.M., Poulton, A.J., Tyrrell, T., Beaufort, L., Dutkiewicz, S., Gibbs, S., Gutowska, M.A., Lee, R., Riebesell, U., Young, J.R., and Ridgwell, A.: Why marine phytoplankton calcify, *Science Advances*, 2, doi: 10.1126/sciadv.1501822, 2016.
- 640 O'Brien, C.J., Peloquin, J.A., Vogt, M., Heinle, M., Gruber, N., Ajani, P., Andrulleit, H., Aristegui, J., Beaufort, L., Estrada, M., Karentz, D., Kocczynska, E., Lee, R., Poulton, A.J., Pritchard, T., and Widdicombe, C.: Global marine plankton functional type biomass distributions: coccolithophores, *Earth System Science Data*, 5, 259-276, doi: 10.5194/essd-5-259-2013, 2013.
- O'Brien, C.J., Vogt, M., and Gruber, N.: Global coccolithophore diversity: Drivers and future change, *Prog. Oceanogr.*, 140, 27-42, doi: 10.1016/j.pocean.2015.10.003, 2016.
- 650 Paasche, E.: Coccolith formation, *Nature*, 193, 1094-1095, doi: 10.1038/1931094b0, 1962.
- Paasche, E.: The adaptation of the carbon-14 method for the measurement of coccolith production in *Coccolithus huxleyi*, *Physiol. Plantarum*, 16, 186-200, 1963.
- 655 Paasche, E.: Adjustment to light and dark rates of coccolith formation, *Physiol. Plant.*, 19, 271-278, 1966.
- Paasche, E.: A review of the coccolithophorid *Emiliania huxleyi* (Prymnesiophyceae), with particular reference to growth, coccolith formation, and calcification-photosynthesis interactions, *Phycologia*, 40, 503-529, 2002.
- 660 Paasche, E., and Brubak, S.: Enhanced calcification in the coccolithophorid *Emiliania huxleyi* (Haptophyceae) under phosphorus limitation, *Phycologia*, 33, 324-330, doi: 10.2216/i0031-8884-33-5-324.1, 1994.
- Poulton, A.J., Sanders, R., Holligan, P.M., Stinchcombe, M.C., Adey, T.R., Brown, L., and Chamberlain, K.: Phytoplankton mineralization in the tropical and subtropical Atlantic Ocean, *Global Biogeochem. Cy.*, 20, GB4002, doi: 10.1029/2006GB002712, 2006.
- 665 Poulton, A.J., Adey, T.R., Balch, W.M., and Holligan, P.M.: Relating coccolithophore calcification rates to phytoplankton community dynamics: Regional differences and implications for carbon export, *Deep-Sea Res. II*, 54, 538-557, doi: 10.1016/j.dsr2.2006.12.003, 2007.
- 670 Poulton, A.J., Charalampopoulou, A., Young, J.R., Tarran, G.A., Lucas, M.I., and Quartly, G.D.: Coccolithophore dynamics in non-bloom conditions during late summer in the central Iceland Basin (July-August, 2007), *Limnol. Oceanogr.*, 55, 1601-1613, doi: 10.4319/lo.2010.55.4.1601, 2010.
- 675 Poulton, A.J., Painter, S.C., Young, J.R., Bates, N.R., Bowler, B., Draeapeau, D., Lyczszkowski, E., and Balch, W.M.: The 2008 *Emiliania huxleyi* bloom along the Patagonian Shelf: Ecology, biogeochemistry, and cellular calcification, *Global Biogeochem. Cy.*, 27, 1023-1033, doi: 10.1002/2013GB004641, 2013.



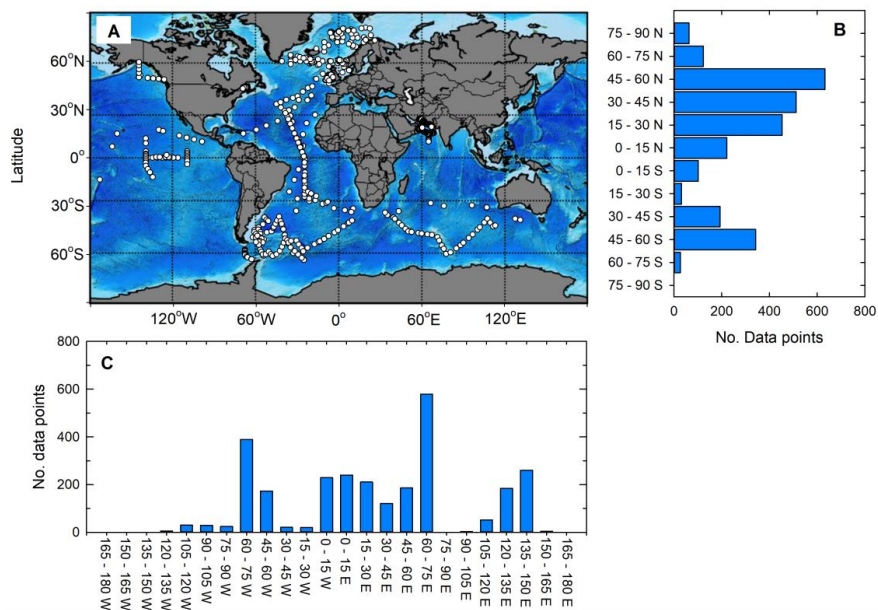
- 680 Poulton, A.J., Stinchcombe, M.C., Achterberg, E.P., Bakker, D.C.E., Dumousseaud, C., Lawson, H.E., Lee, G.A., Richier, S., Suggett, D.J., and Young, J.R.: Coccolithophores on the north-west European shelf: calcification rates and environmental controls, *Biogeosciences*, 11, 3919-3940, doi: 10.5194/bg-11-3919-2014, 2014.
- 685 Poulton, A.J., Holligan, P.M., Charalampopoulou, A., and Adey, T.R.: Coccolithophore ecology in the tropical and subtropical Atlantic Ocean: New perspectives from the Atlantic Meridional Transect (AMT) programme, *Prog. Oceanogr.*, 158, 150-170, doi: 10.1016/j.pocean.2017.01.003, 2017.
- 690 Poulton, A.J., Daniels, C.J., Balch, W.M., Marañón, E., Adey, T., Bowler, B.C., Cermeño, P., Charalampopoulou, A., Crawford, D.W., Drapeau, D.T., Feng, Y., Fernández, A., Fernández, E., Fragoso, G.M., González, N., Graziano, L.M., Heslop, R., Holligan, P.M., Hopkins, J., Huete-Ortega, M., Hutchins, D.A., Lam, P.J., Lipsen, M.S., López-Sandoval, D.C., Loucaides, S., Marchetti, A., Mayers, K.M.J., Rees, A.P., Sobrino, C., Tynan, E., Tyrrell, T.: Global compilation of coccolithophore calcification measurements from unperturbed water samples. PANGAEA, <https://doi.pangaea.de/10.1594/PANGAEA.888182>, 2018.
- 695 Raven, J.A., and Crawford, K.: Environmental controls on coccolithophore calcification, *Mar. Eco. Prog. Ser.*, 470, 137-166, doi: 10.3354/meps09993, 2012.
- 700 Rees, A.P., Woodward, E.M.S., Robinson, C., Cummings, D.G., Tarran, G.A., and Joint, I.: Size-fractionated nitrogen uptake and carbon fixation during a developing coccolithophore bloom in the North Sea during June, 1999, *Deep-Sea Res. II*, 49, 2905-2927, doi: 10.1016/S0967-0645(02)00063-2, 2002.
- 705 Sarmineto, J.L., Dunne, J., Gnanadesikan, A., Key, R.M., Matsumoto, K., and Slater, R.: A new estimate of the CaCO<sub>3</sub> to organic carbon export ratio, *Global Biogeochem. Cy.*, 16, doi: 10.1029/2002GB001919, 2002.
- Schiebel, R.: Planktic foraminiferal sedimentation and the marine calcite budget, *Global Biogeochem. Cy.*, 16, 1065, doi: 10.1029/2001GB001459, 2002.
- Schiebel, R., and Movellan, A.: First-order estimate of the planktic foraminifer biomass in the modern ocean, *Earth Syst. Sci. Data*, 4, 75-89, doi: 10.5194/essd-4-75-2012, 2012.
- 710 Taylor, A.R., Brownlee, C., and Wheeler, G.: Coccolithophore cell biology: Chalking up progress, *Ann. Rev. Mar. Sci.*, 9, 283-310, doi: 10.1146/annurev-marine-122414-034032, 2016.
- 715 Van der Wal, P., Kempers, R.S., and Veldhuis, M.J.W.: Production and downward flux of organic matter and calcite in a North Sea bloom of the coccolithophore *Emiliana huxleyi*, *Mar. Ecol. Prog. Ser.*, 126, 247-265, doi: 10.3354/meps126247, 1995.
- 720 Yool, A., Popova, E.E., and Anderson, T.R.: MEDUSA-2.0: an intermediate complexity biogeochemical model of the marine carbon cycle for climate change and ocean acidification studies, *Geosci. Model Develop.*, 6, 1767-1811, doi: 10.5194/gmd-6-1767-2013, 2013.
- 725 Young, J.R., Davis, S.A., Bown, P.R., and Mann, S.: Coccolith ultrastructure and biomineralisation, *J. Structural Biol.*, 126, 195-215, 1999.
- Young, J.R., and Ziveri, P.: Calculation of coccolith volume and its use in calibration of carbonate flux estimates, *Deep-Sea Res. II*, 47, 1679-1700, doi: 10.1016/S0967-0645(00)0003-5, 2000.
- Young, J.R., Geisen, M., Cross, L., Kleijne, A., Sprengel, C., Probert, I., and Ostergaard, J.: A guide to extant coccolithophore taxonomy, *J. Nanoplank. Res.*, 1, 1-132, 2003.
- 730 Zondervan, I.: The effects of light, macronutrients, trace metals and CO<sub>2</sub> on the production of calcium carbonate and organic carbon in coccolithophores – A review, *Deep-Sea Res. II*, 54, 521-537, 2007.

**Table 1: Data Sources**

| Principal Investigator | Number of CP measurements |              | Region                                       | Method     | Incubation length (hrs) | Cell count method            | Reference(s)  |
|------------------------|---------------------------|--------------|--|------------|-------------------------|------------------------------|---|
|                        | Depth Integrals           | Total Points |  |            |                         |                              |   |
| Balch                  | -                         | 1            | Gulf of Maine                                | Difference | 24                      |                              | Balch et al. (1992)   |
| Balch                  | 11                        | 70           | Equatorial Pacific                           | Difference | 24                      |                              | Balch and Kilpatrick (1996)                                   |
| Balch                  | 51                        | 508          | Arabian Sea                                  | MDT        | 24                      |                              | Balch et al. (2000)   |
| Balch                  | -                         | 492          | Gulf of Maine                                | MDT        | ~12                     | Light microscopy             | Balch et al. (2004); Balch et al. (2008); Balch et al. (2012) |
| Balch                  | 28                        | 157          | Equatorial Pacific                           | MDT        | 24                      |                              | Balch et al. (2011)   |
| Balch                  | 29                        | 153          | Southern Ocean: Atlantic                     | MDT        | 24                      | Light microscopy             | Balch et al. (2016)   |
| Balch                  | 28                        | 145          | Southern Ocean: Indian                       | MDT        | 24                      | Light microscopy             | Balch et al. (2016)   |
| Charalampopoulou       | 6                         | 32           | Arctic Ocean                                 | MDT        | 24                      | Scanning Electron Microscopy | Charalampopoulou et al. (2011)                                |
| Charalampopoulou       | 6                         | 59           | Southern Ocean: Atlantic                     | MDT        | 24                      | Scanning Electron Microscopy | Charalampopoulou et al. (2016)                                |
| Crawford & Lipsen      | 4                         | 21           | Sub-polar North Pacific                      | MDT        | 24                      |                              | Unpublished   |
| Daniels                | -                         | 24           | Arctic Ocean                                 | MDT        | 24                      | Light microscopy             | Daniels et al. (2016)   |
| Daniels & Fragoso      | -                         | 22           | Southern Ocean: Atlantic                     | MDT        | 24                      |                              | Unpublished   |
| Feng                   | -                         | 1            | Sub-polar North Atlantic                     | MDT        | 24                      |                              | Feng et al. (2009)  |
| Fernandez              | 5                         | 28           | Sub-polar North Atlantic                     | Difference | 24                      |                              | Fernandez et al. (1993)                                       |
| Fernandez              | 4                         | 22           | Norwegian Fjord                              | Difference | 24                      |                              | Fernandez et al. (1996)                                       |
| Lam                    | -                         | 1            | Sub-polar North Pacific                      | MDT        | 5                       |                              | Lam et al. (2001)   |
| Lipsen                 | 38                        | 219          | Sub-polar North Pacific                      | MDT        | 24                      | Inverted Light Microscopy    | Lipsen et al. (2007)  |
| Loucaides              | -                         | 18           | Arctic Ocean                                 | MDT        | 24                      | Scanning Electron Microscopy | Unpublished   |
| Marañón                | 2                         | 40           | North Sea                                    | Diff       | 24                      | Haemocytometer               | Marañón and Gonzalez (1997)                                   |
| Marañón                | 1                         | 85           | Tropical Atlantic, Pacific and Indian Oceans | MDT        | 24                      | Inverted Light Microscopy    | Marañón et al. (2016)   |
| Marchetti              | 3                         | 21           | Sub-polar North Pacific                      | MDT        | 24                      |                              | Marchetti et al. (2006)                                       |
| Mayers                 | 6                         | 32           | Celtic Sea                                   | MDT        | 24                      | Light microscopy             | Unpublished   |
| Mayers                 | 8                         | 52           | Celtic Sea                                   | MDT        | 24                      | Light microscopy             | Mayers et al. (2018)  |
| Mayers                 | 7                         | 42           | Celtic Sea                                   | MDT        | 24                      | Light microscopy             | Unpublished   |
| Poulton                | 10                        | 55           | Sub-tropical Atlantic                        | MDT        | 10-16                   |                              | Poulton et al. (2006)   |
| Poulton                | 11                        | 70           | Sub-polar North Atlantic                     | MDT        | 24                      | Light microscopy             | Poulton et al. (2010)   |
| Poulton                | 25                        | 150          | Patagonian Shelf                             | MDT        | 24                      | Light microscopy             | Poulton et al. (2013)   |
| Poulton                | 14                        | 70           | Northwest European Shelf                     | MDT        | 24                      | Light microscopy             | Poulton et al. (2014)   |
| Poulton                | -                         | 17           | Sub-polar North Atlantic                     | MDT        | 24                      | Scanning Electron Microscopy | Unpublished   |
| Poulton & Adey         | -                         | 53           | Sub-tropical Atlantic                        | MDT        | 10-16                   |                              | Poulton et al. (2007)   |
| Rees                   | 9                         | 54           | North Sea                                    | Diff       | 24                      |                              | Rees et al. (2002)  |
| Tynan                  | 4                         | 28           | Arctic Ocean                                 | MDT        | 24                      |                              | Unpublished   |
| Van der Wal            | 4                         | 23           | North Sea                                    | Ca-45      | 24                      |                              | Van der Wal et al. (1995)                                     |
| <b>Total</b>           | <b>314</b>                | <b>2765</b>  |  |            |                         |                              |   |

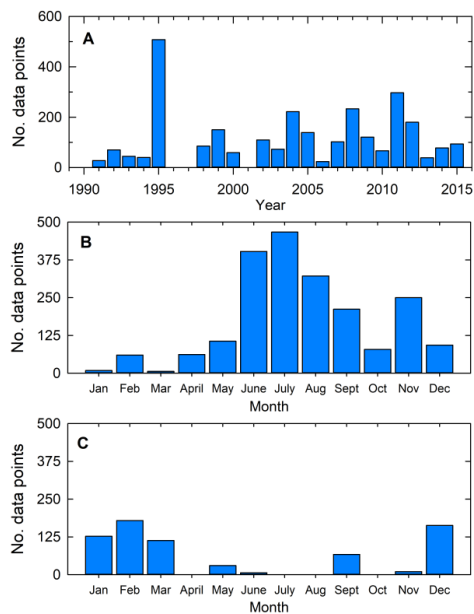


Figures



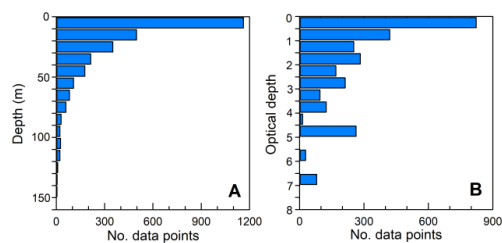
735

**Figure 1: Global map of  $\text{CaCO}_3$  production data (A) and the frequency of data by latitude (B) and longitude (C). Global map in (A) superimposed on ocean bathymetry.**

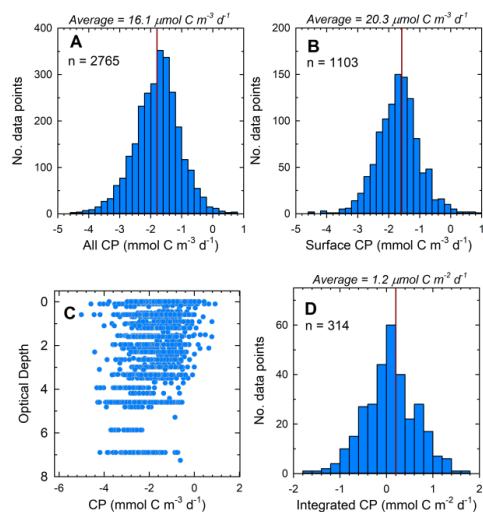


740

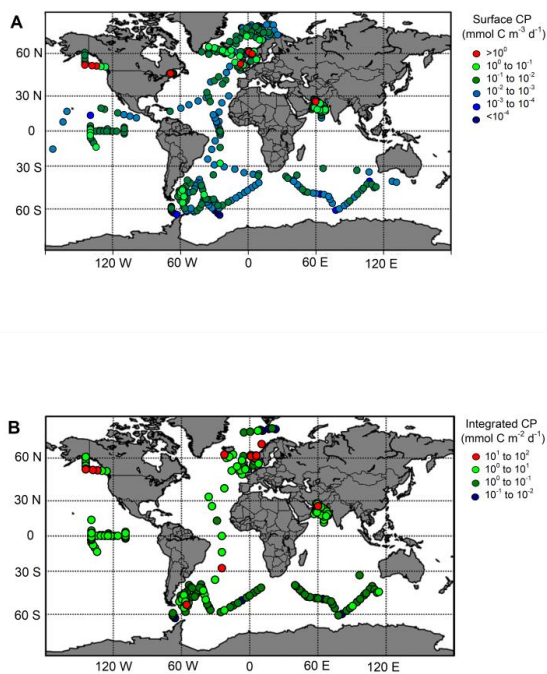
**Figure 2: Frequency of CaCO<sub>3</sub> production data by: (A) year of measurement; (B) month of measurement in the Northern Hemisphere; and (C) month of measurement in the Southern Hemisphere.**



745 **Figure 3: Frequency of CaCO<sub>3</sub> production data by (A) sampling depth, and (B) optical depth. Depths relate to depth of sample collection, not incubation depth.**

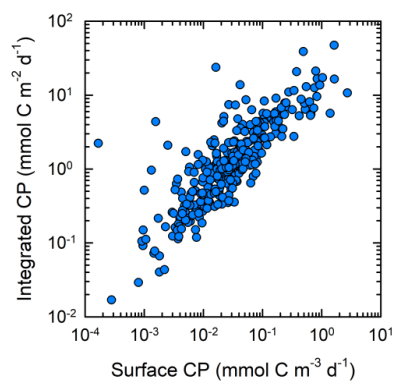


750 **Figure 4: Characteristics of the  $\text{CaCO}_3$  production (CP) database: (A) measurement frequency versus all CP data; (B) measurement frequency for surface CP data only; (C) all CP data versus optical depth; and (D) measurement frequency for euphotic zone integrated CP. Panels (A), (B) and (D) have geometric means presented.**



755

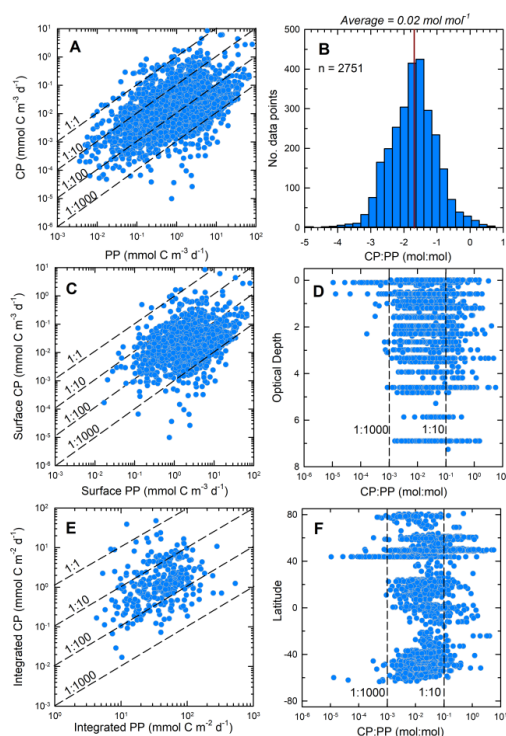
**Figure 5: Global maps of (A) surface CaCO<sub>3</sub> production (CP), and (B) euphotic zone integrated CP. Global maps superimposed on ocean bathymetry as in Fig. 1A.**



760

**Figure 6:** Scatterplot of surface (<20 m) CaCO<sub>3</sub> production (CP) and euphotic zone integrated CP. The relationship between the two is statistically significant (Pearson's product-moment correlation,  $r = 0.83$ ,  $p < 0.001$ ,  $n = 314$ ).

765



770 **Figure 7: Characteristics of the relationship between  $\text{CaCO}_3$  production (CP) and Primary production (PP):** (A) scatterplot of all CP and PP data; (B) frequency histogram of CP to PP ratios for all data; (C) scatterplot of only surface (<20 m) CP and PP; (D) scatter plot of CP:PP ratios against optical depth; (E) scatterplot of euphotic zone integrals of CP and PP; and (F) scatter plot of CP:PP ratios by latitude. Panels (A, C, D, E, F) include dashed lines of constant CP:PP. Panel (B) has the geometric mean ratio of CP to PP for all data indicated.

775

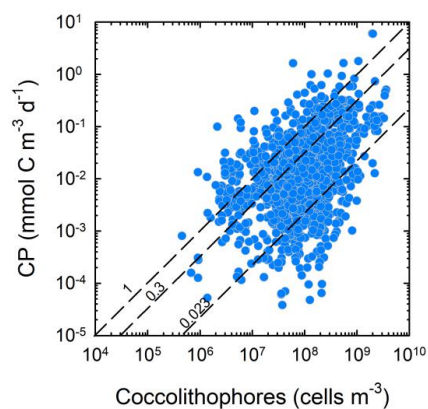


**Figure 8:** Scatterplot of coccolithophore cell abundances and  $\text{CaCO}_3$  production (CP) for all samples with matched count and rate data. Dashed lines indicate representative lines of cell-specific calcification (see Sect. 3.4).

780



## Appendix A

In summer 2010, during a research cruise to the North Atlantic (*RRS Discovery*, 4<sup>th</sup> July to 11<sup>th</sup> August, D354) seawater samples were collected and analysed using both the difference technique (Diff) and the Micro-Diffusion  
785 Technique (MDT). Seawater for these comparisons was collected from sites ( $n = 19$ ) in the Iceland and Irminger basins from sub-surface (~5 m) waters during pre-dawn (06:00-07:00 h local time) deployments of a titanium CTD fitted with 10 L Niskin bottles on a rosette sampler.

For the MDT, 150 mL water samples (3 light, 1 formalin-killed) were spiked with 25 to 56  $\mu\text{Ci}$  (925-2,072 kBq) of  $^{14}\text{C}$ -labelled sodium bicarbonate (Perkin-Elmer, UK) and incubated in on-deck incubators chilled with sea-  
790 surface seawater and with irradiance levels replicating ~30 to 40% of surface incidental irradiance using misty blue light filters (Lee Filters<sup>TM</sup>, UK). Incubations were terminated after 24 h by filtering through 25 mm 0.2  $\mu\text{m}$  polycarbonate filters, with extensive rinsing with fresh filtered seawater to remove any labelled  $^{14}\text{C}$ -DIC. Full methodology followed Poulton et al. (2010, 2013, 2014) and gave measurements of primary production ( $\text{PP}_{\text{MDT}}$ )  
795 and  $\text{CaCO}_3$  production ( $\text{CP}_{\text{MDT}}$ ). The average coefficient of variation of triplicate (light)  $\text{PP}_{\text{MDT}}$  measurements was 2% (10 to 28%) and 19% (1 to 72%) for  $\text{CP}_{\text{MDT}}$ , across a range of  $\text{PP}_{\text{MDT}}$  from 1.5 to 5.3  $\text{mmol C m}^{-3} \text{d}^{-1}$ .

In parallel to the MDT measurements, measurements were also made of total particulate production (TPP) and primary production ( $\text{PP}_{\text{Diff}}$ ), with the difference between the two being taken as  $\text{CaCO}_3$  production (i.e.,  $\text{CP}_{\text{Diff}} =$   
800  $\text{TPP} - \text{PP}_{\text{Diff}}$ ), following the general methodology of Fernández et al. (1993) and Balch et al. (2000). Two slightly different protocols were used: for five experiments, TPP and  $\text{PP}_{\text{Diff}}$  were measured from separate bottles, while for fourteen experiments, TPP and  $\text{PP}_{\text{Diff}}$  were measured from the same bottle. Formalin-killed blanks were prepared in only seven experiments, with formalin values averaged and the average applied across the other twelve experiments. (Note: formalin-killed blank values were, on average, only ~4% of TPP and  $\text{PP}_{\text{Diff}}$  values (range 2%  
805 to 6% for both)).

Water samples (150 mL, 3 or 6 or 7) were collected, spiked with 3 to 13  $\mu\text{Ci}$  (108 to 489 kBq) of  $^{14}\text{C}$ -labelled sodium bicarbonate (Perkin-Elmer, UK) and incubated in parallel to the MDT samples. Incubations were terminated after 24 h with filtering through 25 mm 0.2  $\mu\text{m}$  polycarbonate filters, with extensive rinsing with fresh  
810 filtered seawater to remove any labelled  $^{14}\text{C}$ -DIC. Filters for the measurement of TPP were placed directly into scintillation cocktail after air-drying, while filters for  $\text{PP}_{\text{Diff}}$  were either acid-fumed (hydrochloric acid, 2-3 h) or had 1 mL of 1% phosphoric acid added (20-24 h). The average coefficient of variation of the triplicate TPP measurements was 13% (1 to 27%) and 15% (4 to 21%) for  $\text{PP}_{\text{Diff}}$ , across a range of  $\text{PP}_{\text{Diff}}$  from 1.4 to 2.9  $\text{mmol C m}^{-3} \text{d}^{-1}$ . (Note. The standard errors on the triplicate TPP measurements range from 95 to 1294  $\mu\text{mol C m}^{-3} \text{d}^{-1}$ ,  
815 while the standard errors for  $\text{PP}_{\text{Diff}}$  range from 31 to 804  $\mu\text{mol C m}^{-3} \text{d}^{-1}$ ; these values are comparable to the higher end of CP measured in the open-ocean, see main paper).

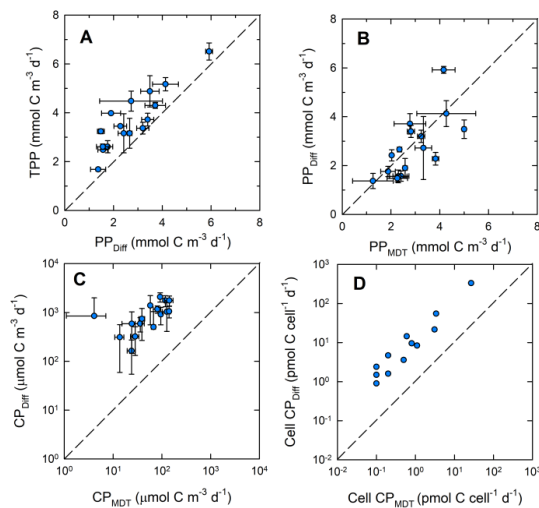
Comparison of TPP and  $\text{PP}_{\text{Diff}}$  (Fig. S1A) showed that the two are significantly positively correlated ( $r = 0.89$ ,  $p < 0.001$ ,  $n = 15$ ), though  $\text{PP}_{\text{Diff}}$  tended to be, on average, ~27% (5 to 54%) lower than TPP.  $\text{PP}_{\text{Diff}}$  and  $\text{PP}_{\text{MDT}}$  are also closely correlated (Fig. S1B;  $r = 0.71$ ,  $p < 0.005$ ) with the average difference being only ~7% (although  
820



differences did span -27% to 45%). However, TPP being around a third higher than  $PP_{\text{Diff}}$  actually implies that rates of  $CP_{\text{Diff}}$  ( $= TPP - PP_{\text{Diff}}$ ) range from 164 to 2081  $\mu\text{mol C m}^{-3} \text{d}^{-1}$  (Fig. S1C), with a cruise average of 952  $\mu\text{mol C m}^{-3} \text{d}^{-1}$ . In contrast,  $CP_{\text{MDT}}$  only ranged from 4.1 to 141.8  $\mu\text{mol C m}^{-3} \text{d}^{-1}$  (with a cruise average of 68  $\mu\text{mol C m}^{-3} \text{d}^{-1}$ ), which is ~60 to ~9000 times lower than  $CP_{\text{Diff}}$  (Fig. S1C), though the two are significantly correlated ( $r = 0.69, p < 0.005, n = 15$ ). Since  $PP_{\text{Diff}}$  and  $PP_{\text{MDT}}$  are strongly correlated, with a low relative difference between the two, the discrepancy between  $CP_{\text{Diff}}$  and  $CP_{\text{MDT}}$  derives from the much higher measurement of TPP. At this time there are no clear explanations for why TPP is so high relative to PP. It may be speculated that it is linked to the treatment of the samples (air-drying), as both PP measures are exposed to acid, and hence an unidentified source of labelled-carbon may be included in the TPP measurement but not those of PP. Further comment is outside the scope of this study.

Objectively determining which CP measurement is accurate is not straightforward. One way is to consider the cell-normalised rates of calcification (cell-CP); i.e. which set of CP gives physiologically realistic cell-CP? For example, based on culture and field data *Emiliania huxleyi* may have cell-CP of 0.1 to 1.0  $\text{pmol C cell}^{-1} \text{d}^{-1}$  (see discussion in Poulton et al., 2010, 2013 and references therein, also Daniels et al., 2014). Maximum cell-CP for heavier species such as *Coccolithus pelagicus* may reach as high as ~8.3  $\text{pmol cell}^{-1} \text{d}^{-1}$  or ~23.2  $\text{pmol C cell}^{-1} \text{d}^{-1}$  for *C. braarudii* (depending on cell calcite and growth rates; Daniels et al., 2014). For the 2010 North Atlantic data, calculated cell-CP ( $n = 12$ ) for  $CP_{\text{Diff}}$  gives a range of cell-CP of 0.5 to 55.2  $\text{pmol C cell}^{-1} \text{d}^{-1}$  (geometric mean = 4.40  $\text{pmol C cell}^{-1} \text{d}^{-1}$ ), while for  $CP_{\text{MDT}}$  a lower range of 0.02 to 3.36  $\text{pmol C cell}^{-1} \text{d}^{-1}$  (geometric mean = 0.25  $\text{pmol C cell}^{-1} \text{d}^{-1}$ ) is calculated. Generally, cell-CP from  $CP_{\text{Diff}}$  is on average 32 times higher (full range 7-206) than cell-CP calculated from  $CP_{\text{MDT}}$ . Cell-CP from the MDT gives values more in line with similar studies in the literature, although clearly further details of the species composition of the community (relative abundance, calcite content and growth rates) is required to fully reconcile the different estimates of cell-CP.

To conclude, the MDT provided CP and cell-CP rates which are fully consistent with the database and wider literature, whereas the Diff technique provides CP rates which are much higher than those most often found in non-bloom conditions in the North Atlantic and cell-CP rates which are high. Based on these observations, we suggest that the MDT is used for further field studies and the Diff technique is reserved for culture-based studies.



850

855

**Figure A1: Scatterplots of:** (A) total particulate production (TPP) and primary production from the difference technique ( $PP_{Diff}$ ); (B) primary production from the Micro-Diffusion Technique ( $PP_{MDT}$ ) and difference method ( $PP_{Diff}$ ); (C)  $CaCO_3$  production from the Micro-Diffusion Technique ( $CP_{MDT}$ ) and difference method ( $CP_{Diff}$ ); and (D) cell-normalised rates (cell-CP) from the Micro-Diffusion Technique (Cell- $CP_{MDT}$ ) and difference method (Cell- $CP_{Diff}$ ). Dashed lines in all panels indicate unity.